New Journal of Physics
The open-access journal for physics

Acoustic transparency in two-dimensional sonic crystals

José Sánchez-Dehesa[1,3], Daniel Torrent[1] and Liang-Wu Cai[2]

[1] Wave Phenomena Group, Department of Electronic Engineering, Polytechnic University of Valencia, C/ Camino de Vera s/n, E-46022 Valencia, Spain

[2] Department of Mechanical and Nuclear Engineering, Kansas State University, Manhattan, KS 66506, USA

E-mail: jsdehesa@upvnet.upv.es

New Journal of Physics **11** (2009) 013039 (12pp)
Received 22 September 2008
Published 23 January 2009
Online at http://www.njp.org/
doi:10.1088/1367-2630/11/1/013039

Abstract. Acoustic transparency is studied in two-dimensional sonic crystals consisting of hexagonal distributions of cylinders with continuously varying properties. The transparency condition is achieved by selectively closing the acoustic bandgaps, which are governed by the structure factor of the cylindrical scatterers. It is shown here that cylindrical scatterers with the proposed continuously varying properties are physically realizable by using metafluids based on sonic crystals. The feasibility of this proposal is analyzed by a numerical experiment based on multiple scattering theory.

Contents

[3] Author to whom any correspondence should be addressed.

1. Introduction

The prospect of designing artificial electromagnetic (EM) materials with physical properties unavailable in natural materials, such as negative refraction index, has opened a new field of research named EM metamaterials. An EM metamaterial consists of a set of subwavelength EM units and their extraordinary properties are determined by the geometric arrangement and intrinsic properties of the building EM units. Recently, EM metamaterials having a negative refraction index, making a given object transparent to the impinging radiation have been reported [1, 2], and certain proposed designs have also been experimentally realized [3].

In acoustics, the analogous topics such as negative refraction index [4] and acoustic transparency [5] have also been investigated because of fundamental importance as well as their potential applications. Acoustic transparency has been predicted under very restrictive conditions for a single-layered sphere [5]; full transparency was only predicted for a single frequency at a specifically designed combination of materials and geometrical arrangement.

In this work, we show that full acoustic transparency can be achieved in a preselected range of frequencies by using a two-dimensional (2D) sonic crystal (SC) with a periodic distribution of acoustic scatterers in which each scatterer is a layered fluidlike cylinder. A mechanism of switching off the SC bandgaps at the pre-selected frequency range is utilized to achieve the acoustic transparency. Here, bandgap closing is achieved by tuning the refractive index of the host in which the layered fluidlike scatterers are embedded. We also propose a scheme for the actual realization of the systems under study by engineered acoustic metamaterials or metafluids that exhibit the desired properties.

2. Theory

Let us start with the propagation of longitudinal waves in a periodic 2D fluid–fluid system. For plane waves of frequency ω, the scalar acoustic pressure field $p(\mathbf{r})$ characterizing those waves satisfies the wave equation

$$\nabla \cdot \left(\frac{\nabla p(\mathbf{r})}{\rho(\mathbf{r})} \right) + \frac{\omega^2}{\lambda(\mathbf{r})} p(\mathbf{r}) = 0, \tag{1}$$

where $\rho(\mathbf{r})$ and $\lambda(\mathbf{r})$ are functions representing the density and the local bulk elasticity modulus, respectively, at the spatial location $\mathbf{r}$. Both functions have the periodicity of the corresponding Bravais lattice. They define the sound speed in the system, $c(\mathbf{r}) = \sqrt{\lambda(\mathbf{r})/\rho(\mathbf{r})}$. Moreover, inside each unit cell in the lattice, we assume that each scatterer is a layered cylinder whose acoustic parameters exhibit a certain radial dependencies $\rho_s(r')$ and $\lambda_s(r')$, where r' is measured from the cylinder center, and it is embedded in a uniform background with parameters ρ_0 and λ_0.

For simplicity, we assume here that scatterers and background have the same density $\rho_s(r) = \rho_0$. Results for the general case in which the background density and bulk modulus are different from those of the scatterers could be obtained but they are out of the scope of the present work. The chosen simplifying assumption has the advantage of being physically realizable by using recently proposed acoustic metamaterials [6]. Therefore, for the system studied here, equation (1) can be cast into the Helmholtz equation [7]

$$\left[\nabla^2 + F(\mathbf{r}) \right] p(\mathbf{r}) = 0, \tag{2}$$

where

$$F(\mathbf{r}) = n^2(\mathbf{r})\frac{\omega^2}{c_\mathrm{b}^2} \tag{3}$$

is a periodic function of $\mathbf{r}$ with periodicity $\mathbf{R} = m_1\mathbf{a} + m_2\mathbf{b}$, where $\mathbf{a}$ and $\mathbf{b}$ are the primitive vectors of the corresponding Bravais lattice and m_i are integers. This function expresses the periodic changes of the refractive index $n(\mathbf{r}) = c_\mathrm{b}/c(\mathbf{r})$ in terms of periodic fluctuation of the eigenvalues of the Helmholtz equation. Let us stress that, inside each unit cell, $n(\mathbf{r})$ has a radial dependence $n_\mathrm{s}(r')$ associated with the layered scatterers and it is unity in the background. It is interesting to point out that, for the limiting case where the scatterers behave like δ functions, the explicit form of $F(\mathbf{r})$ will be

$$F(\mathbf{r}) = \frac{\omega^2}{c_\mathrm{b}^2}[1 + g\Omega_0 \sum_{\mathbf{R}} \delta(\mathbf{r} - \mathbf{R})], \tag{4}$$

where g is a measure of the strength of the scatterer located at $\mathbf{R}$, and Ω_0 is the volume of the unit cell.

Equation (2) is equivalent to the stationary Schrodinger equation with potential U and energy E such that

$$U - E = -\frac{n^2(\mathbf{r})}{2}. \tag{5}$$

Therefore, we expect that acoustic scattering of sound waves is equivalent to scattering of electronic waves in solids having the potential (5).

2.1. Transparency conditions for SCs

Our system of periodic distribution of fluid scatterers embedded in a fluid background defines a SC in which the sound waves, like the electronic waves propagating in solids, will experience a Bragg diffraction by all parallel planes in the crystalline structure. Let us recall that every reciprocal lattice vector $\mathbf{G}_{hk}$ is normal to a lattice plane of the crystal structure. Thus, the reciprocal lattice vector $\mathbf{G}_{hk} = h\mathbf{A} + k\mathbf{B}$, where $\mathbf{A}$ and $\mathbf{B}$ are the primitive vectors of the reciprocal lattice, is normal to the plane in the crystal structure defined by the Miller indices (h, k) [8], where h and k are integers.

According to scattering theory derived in solid-state physics [8], the amplitude of all the reflections (hk) possible for a given crystal lattice is determined by the so-called structure factor. For the case of scattering of sound waves, we introduce the equivalent quantity $S(\mathbf{G}_{hk})$ as follows:

$$S(\mathbf{G}_{hk}) \equiv \frac{1}{\Omega_0}\int_{\Omega_0} \mathrm{d}\mathbf{r}\, n^2(\mathbf{r})\mathrm{e}^{-\mathrm{i}\mathbf{G}_{hk}\cdot\mathbf{r}}. \tag{6}$$

The transparency regime (i.e. non-diffraction condition for any propagating wave) is achieved by applying the vanishing condition over the lattice structure, i.e. $S(\mathbf{G}_{hk}) = 0$ for every reciprocal vector $\mathbf{G}_{hk}$. This condition gives a requirement of the elasticity modulus, which is the only variable for the acoustic system under consideration:

$$\int_{\Omega_0}\left(\frac{1}{\lambda_\mathrm{s}(r)} - \frac{1}{\lambda_\mathrm{b}}\right)\Theta(r_\mathrm{s} - r)\exp\left(-\mathrm{i}\mathbf{G}_{hk}\cdot\mathbf{r}\right)\,\mathrm{d}\mathbf{r} = 0, \quad (|\mathbf{G}_{hk}| \neq 0), \tag{7}$$

where r_s is the cylinder radius and $\Theta(x)$ is defined such that $\Theta(x) = 1$ for $x \geqslant 0$ and $\Theta(x) = 0$ for $x < 0$,

Note that when condition (7) is selectively applied over a given reciprocal lattice G_{hk}, the disappearance of the stop band associated to the (hk) Bragg plane is achieved and total transparency at the corresponding range of frequencies will be obtained (see the discussion in the next subsection). However, for stop bands originating from overlapping different $\mathbf{G}_{hk}$ planes, the transparency condition should be carefully obtained.

By integrating with respect to the angular variable in the polar coordinate system, we can obtain the requirement on the background elasticity modulus that satisfies the transparency condition:

$$\frac{1}{\lambda_b^0} = \frac{\int_0^{r_s} (r/\lambda_s(r)) J_0(G_{hk} r)\, \mathrm{d}r}{\int_0^{r_s} r\, J_0(G_{hk} r)\, \mathrm{d}r}, \tag{8}$$

where $G_{hk} \equiv |\mathbf{G}_{hk}|$. Therefore, for a given profile $\lambda_s(r)$, the transparency conditions (8) will be different for different crystalline structures. For a binary system, when $\lambda_s(r) = \lambda_s = \text{constant}$, the condition above reduces to the trivial solution $\lambda_b^0 = \lambda_s$. In the discussion that follows, we consider $1/\lambda_b^0$ as a continuous function of its argument G_{hk}.

To observe the general features of transparency in a SC made of layered fluidlike scatterers, one should study the transparency (non-diffraction) conditions for various lattice arrangements and refractive index profiles $n_s(r)$ in a large range of G. As an example, we analyze cylinders of continuously varying properties of radius $r_c = 0.3a$, where a is the parameter of an hexagonal lattice where primitive vectors are $\mathbf{a} = a(1, \sqrt{3})/2$ and $\mathbf{b} = a(-1, \sqrt{3})/2$. The primitive vectors of the reciprocal lattice are, respectively, $\mathbf{A} = 2\pi(1, 1/\sqrt{3})/a$ and $\mathbf{B} = 2\pi(-1, 1/\sqrt{3})/a$. In order to derive an analytical expression from (8), we consider the following two simple profiles:

$$n_s(r) = \left[n_0^2 + (n_f^2 - n_0^2)(r/r_s)^2\right]^{1/2} \tag{9}$$

$$n_s(r) = \left[n_0^2 + (n_f^2 - n_0^2)(r/r_s)\right]^{1/2} \tag{10}$$

where n_0 and n_f represent the refractive indices at the cylinder center $[n_0 = n_s(0)]$ and its edge $[n_f = n_s(r_s)]$, respectively. Since $n_s(r) = [\lambda_b/\lambda_s(r)]^{1/2}$, the profiles $\lambda_s^{-1}(r)$ to be introduced in (8) are of low powers of (r/r_s):

$$\lambda_s^{-1}(r) = \frac{1}{\lambda_b}\left[n_0^2 + (n_f^2 - n_0^2)(r/r_s)^2\right], \tag{11}$$

$$\lambda_s^{-1}(r) = \frac{1}{\lambda_b}\left[n_0^2 + (n_f^2 - n_0^2)(r/r_s)\right] \tag{12}$$

that can be easily integrated.

Equation (8) is solved for two profiles of type (9) and two of type (10), all of which are depicted in figure 1. Figure 2 shows the solutions for these profiles and they are depicted with the same colors as those used in figure 1. For example, the solid black curve represents the profile of type (9) with $n_0 = 1$ and $n_f = 2.23$. The solution to (8) for this particular profile is represented by the solid black curve in figure 2.

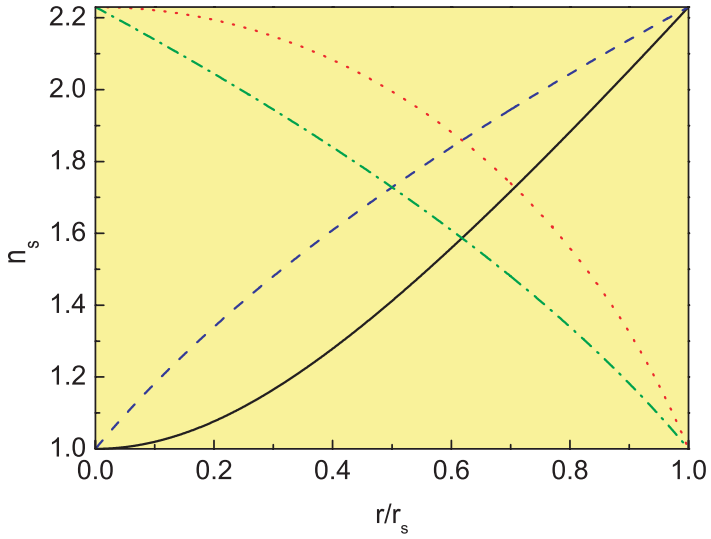

Figure 1. The profiles of acoustic refractive index $n_s(r)$ studied in this work. They have a radial dependence following equations (9) and (10). The solid black curve and the dashed blue curve represent the profiles given by (9) and (10) in which the refractive index at the scatterer center is equal to that of the background [i.e. $n_s(r=0) \equiv n_0 = 1$] and $n_s(r=r_s) \equiv n_f = 2.23$ at its edge. The other two curves are such that $n_0 = 2.23$ and $n_f = 1$; the dotted red curve was obtained from (9) while the dashed-dotted green curve was obtained from (10).

The vertical lines in figure 2 represent the moduli of the reciprocal vectors of the hexagonal lattice,

$$G_{hk} = (4\pi/\sqrt{3})a^{-1}\sqrt{h^2+k^2-hk}. \tag{13}$$

Therefore, the intersection of the vertical lines with the curves in figure 2 define the values of $(\lambda_b^0)^{-1}$ at which the transparency condition is achieved. The open circles in this figure indicate the intersection points for the case of the profile defined by the black line.

In comparison with simple binary systems, results in figure 2 show that any inhomogeneity within the scatterers produces a variation of λ_b^0 depending on G, i.e. in a variation of the bandgap closing condition for different (hk) Bragg bandgap. Also note in figure 2 that $(\lambda_b^0)^{-1}(G)$ shows a quasi-periodic behavior with relevant resonance features at $G = G_{res}$, where G_{res} are determined by requiring the denominator of (8) to vanish. When a Bragg plane (hk), like G_{21}, is located near a resonance of $(\lambda_b^0)^{-1}(G)$, the associated Bragg diffraction cannot be suppressed. Let us stress that, at G_{res}, the transparency condition is not satisfied at any profile $n_s(r)$ here analyzed and the background modulus. Moreover, for any reciprocal vector away from the resonance ($G \neq G_{res}$) and any physically feasible profile of $n_s(r')$ one can find an embedded medium with modulus $(\lambda_b^0)^{-1}(G)$ allowing the suppression of the (hk) Bragg bandgap so that the resultant SC becomes acoustically transparent at the corresponding wavelength.

It can also be concluded from figure 2 that for all the profiles studied here, the suppression of the Bragg bandgaps depends only on the modulus of the associated reciprocal vectors. For example, the closing of bandgap associated with G_{10} and G_{11} is predicted at the same value, i.e. at $(\lambda_b^0)^{-1}(10) = 2.42/\lambda_b$, which is defined by an open circle. This result is further analyzed in the next subsection.

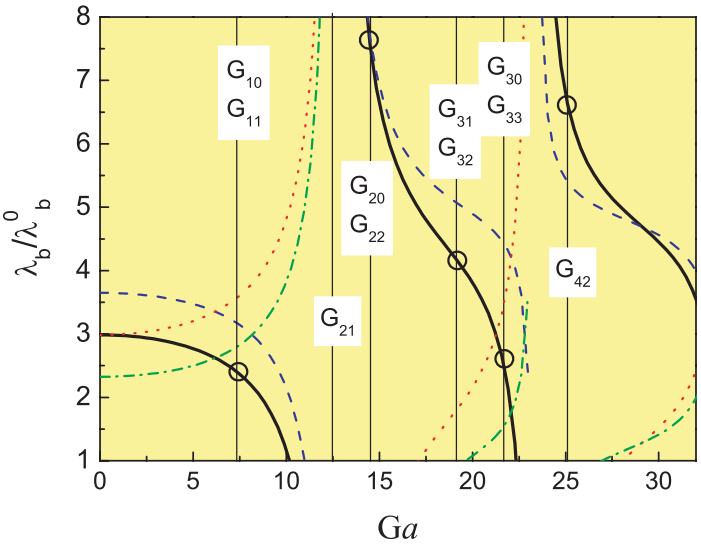

Figure 2. The transparency conditions for a two-dimensional SC consisting of a hexagonal lattice of cylindrical scatterers with the radially varying refractive index profile $n_s(r)$ depicted in figure 1. The different curves represent the condition over the elasticity modulus of the background $\lambda_b^0(G)$ that verify the transparency (non-diffraction) condition in (7). They are plotted as a function of a continuously varying reciprocal wave vector, G, times the lattice parameter a. The vertical lines define the values of the reciprocal vectors (see (13)) that are written over the lines. The hollow circles over the black line define the non-diffraction condition corresponding to a piecewise-parabolic profile $\lambda_s^{-1}(r)$ (see (11)) with a denser near-surface region gives values (hollow circles) $(\lambda_b^0)^{-1}(10) = 2.42/\lambda_b$, $(\lambda_b^0)^{-1}(20) = 7.69/\lambda_b$, $(\lambda_b^0)^{-1}(31) = 4.10/\lambda_b$, $(\lambda_b^0)^{-1}(30) = 2.86\lambda_b$, and $(\lambda_b^0)^{-1}(42) = 6.63/\lambda_b$.

2.2. Transparency versus bandgap closing

The transparency conditions in (7) have been obtained by imposing the condition so that the sound waves traveling through the SC are not diffracted by the scatterer array. In what follows, we correlate the non-diffraction condition with the simultaneous closing of the bandgaps in the acoustic band structure. Particularly, we analyze the case of the first bandgaps appearing along the two high symmetry directions in the hexagonal lattice ΓJ and ΓX.

We follow here a procedure similar to the one that was previously used to analyze an equivalent problem in 2D photonic crystals [9, 10]. Group theory can be applied to obtain analytical formulas that give the acoustic bandedges in terms of Fourier expansion coefficients Λ of the bulk modulus

$$\lambda(\mathbf{r}) = \sum_{\mathbf{G}_{hk}} \Lambda(\mathbf{G}_{hk}) e^{i\mathbf{G}_{hk}\cdot\mathbf{r}}, \tag{14}$$

where

$$\Lambda(\mathbf{G}_{hk}) = \frac{1}{\Omega_0} \int_{\Omega_0} \lambda(\mathbf{r}) e^{-i\mathbf{G}_{hk}\cdot\mathbf{r}}. \tag{15}$$

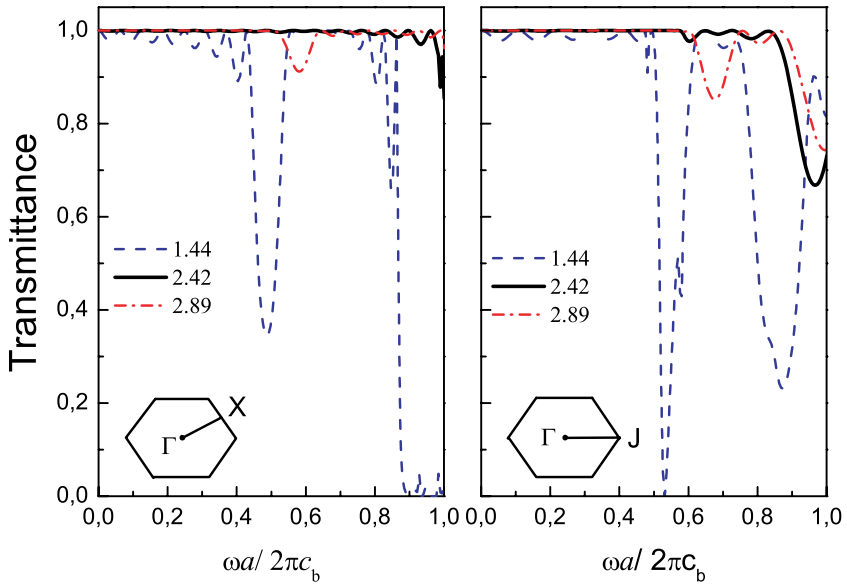

Figure 3. Multiple scattering calculation of the transmittance through a slab made of eight layers of cylinders orientated along the two high-symmetry directions of the hexagonal lattice, ΓX (left panel) and ΓJ (right panel), respectively. The cylinders in the slab have equal radii $r_c = 0.3a$, where a is the lattice parameter. Each cylinder is a layered fluidlike composite defined by an index of refraction $n_s(r)$ given by (9) and their mass density is equal to that of the background. Results are shown for several values of the ratio λ_b/λ_b^0.

These Fourier transformations can be easily calculated by recalling that

$$\lambda(\mathbf{r}) = \lambda_b + \sum_{\mathbf{R}} \lambda(\mathbf{r} - \mathbf{R}), \tag{16}$$

and inside each unit cell $\lambda(\mathbf{r}') = [\lambda_s(r') - \lambda_b]\Theta(r_s - r')$. Because of the radial dependence of $\lambda(\mathbf{r})$ the Fourier coefficients depend only on the modulus of the reciprocal vectors G_{hk}.

The procedure starts by examining the free acoustic modes for the 2D hexagonal lattice following the procedure developed in the study of the electronic band structures. Afterwards, we study the bandgaps near the lowest free acoustic modes at the main points of the first Brillouin zone (BZ). For example, the threefold degeneracy existing in homogeneous fluid would be split into two states P_1 and P_3 with different frequencies. We use symmetrized linear combinations of plane waves that transform like the rows of the irreducible representations to get the basis in which the differential equation is automatically diagonal. In comparison with the case of the 2D photonic band structure an exact duality exists between the photonic modes with E polarization and the acoustic modes under the variable exchange $[p, \mathbf{v}, \rho, \lambda^{-1}] \leftrightarrow [-E_z, \mathbf{H}, \mu, \epsilon]$. This duality is corroborated by our findings below. Thus for the first bandgap at the J point of the hexagonal BZ (see inset in figure 3)

$$\omega_1^2(J) = (\Lambda_0 + 2\Lambda_1)\, \nu_0 |\mathbf{k}_J|^2, \tag{17a}$$

$$\omega_3^2(J) = (\Lambda_0 - \Lambda_1)\, \nu_0 |\mathbf{k}_J|^2, \tag{17b}$$

where $\mathbf{k}_J = (2\pi/a)(2/3, 0)$ is the wavevector of J and Λ_0 and ν_0 are the average bulk modulus and the inverse of the mass density, respectively. $\Lambda_1 = \Lambda(G_1)$, where $G_1 = 4\pi/a\sqrt{3}$ is from (13) the modulus of both vectors $\mathbf{G_{01}}$ and $\mathbf{G_{11}}$.

By following a similar procedure, at the X point,

$$\omega_1^2(X) = (\Lambda_0 + \Lambda_1)\,\nu_0|\mathbf{k}_X|^2, \tag{18a}$$

$$\omega_2^2(X) = (\Lambda_0 - \Lambda_1)\,\nu_0|\mathbf{k}_X|^2, \tag{18b}$$

where $\mathbf{k}_X = (2\pi/a)(\frac{1}{2}\sqrt{3}, \frac{1}{2})$.

Now, the difference between the squared frequencies at J and X points,

$$\omega_3^2(J) - \omega_1^2(J) = -3\Lambda_1\nu_0 k_J^2, \tag{19a}$$

$$\omega_2^2(X) - \omega_1^2(X) = -\Lambda_1\nu_0 k_X^2. \tag{19b}$$

At this point, it is important to remark that all these analytical expressions are valid only up to the first order in the theory of perturbations. In other words, we have explicitly assumed that we are working with dilute systems or a low mismatch of refractive indices between scatterers and the background. Under these conditions, it can be demonstrated that the transparency conditions obtained from the general equation (6) are the same as the bandgap closing conditions obtained from (15), i.e. $\Lambda(\mathbf{G}_{hk}) = 0$ for every reciprocal vector $\mathbf{G}_{hk}$.

To conclude, note that the splitting at both high-symmetry points only depends on Λ_1 and, therefore, the bandgaps associated with Bragg planes G_{01} and G_{11} will be closed simultaneously as was predicted by the non-diffraction condition (see figure 2).

3. Numerical simulations

3.1. Calculation of the transmittance spectra

To verify the theoretical predictions discussed above, we study first the transmittance through a SC slab consisting of eight layers of cylinders with radially varying acoustic properties. As an example, we present results for cylinders defined by profile (9) with $n_0 = 1$ and $n_f = 2.23$ (black curve in figure 1). The transmission spectra have been calculated by developing an algorithm similar to that employed by Yasumoto *et al* [11] in the propagation of EM waves through layers of dielectric scatterers. It is explicitly assumed that the layers are infinitely long in the transversal direction.

The transmittance has been calculated for two different configurations of the slab. In the first configuration, we assume that the layers grow along the ΓX-direction of the BZ. In the second configuration, the growing direction is the ΓJ-direction. Both spectra were calculated by using the vanishing condition $(\lambda_b^0)^{-1} = 2.42/\lambda_b$ determined from (8) and depicted as black lines in separated panels in figure 3. The spectra for two more values, $(\lambda_b^0)^{-1} = 1.44/\lambda_b$ (blue dashed line) and $(\lambda_b^0)^{-1} = 2.89/\lambda_b$ (red dashed-dotted line), are also shown in figure 3. The comparison between spectra indicates that dips in transmission spectra appearing in the low-frequency range completely disappear in the transmittance spectra corresponding to the vanishing condition (black line). Those transmission dips are associated with the first bandgaps existing along the high-symmetry directions in the BZ (i.e. ΓJ and ΓX, respectively) as will be discussed in the next subsection.

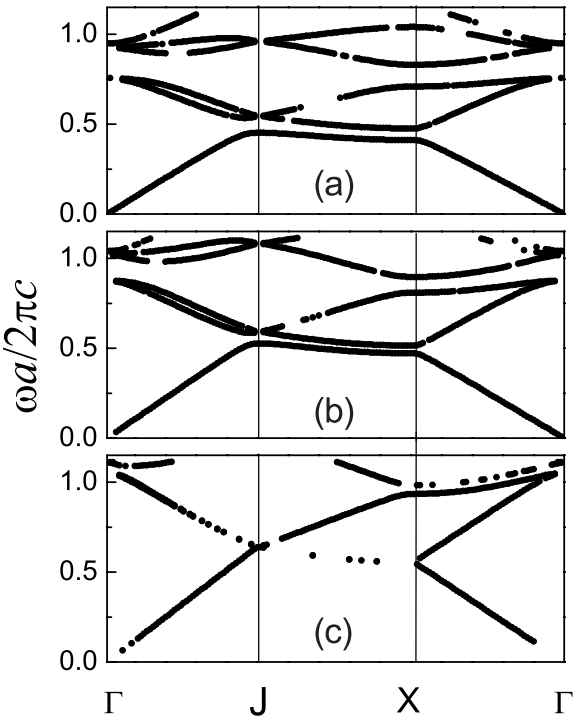

Figure 4. Acoustic bands obtained by multiple scattering simulations. They correspond to SCs based on layered cylinders put in a hexagonal lattice with parameter a. The cylinders of radii $r_s = 0.3a$ are characterized by a radial refractive index $n_s(r) = \sqrt{1 + 3.97(r/r_s)^2}$ (black curve in figure 1) embedded in a background with elastic modulus (a)$\lambda_b^0 = \lambda_b$, (b) $1/\lambda_b^0 = 1.44/\lambda_b^0$, and (c)$1/\lambda_b^0 = 2.42/\lambda_b$.

3.2. Band structure calculation

The acoustic band structures for the corresponding infinite systems have also been calculated in the framework of multiple scattering theory. In brief, the acoustic band structure has been obtained by solving the secular equation that results from applying the Bloch theorem to the multipole coefficients defining the expansion of the scattered pressure. Details of the mathematical procedure can be found in [12].

Figure 4 represents the acoustic bands calculated for the same kind of layered cylinder studied in figure 3 and for three different values of the background modulus λ_b^0.

Figure 4 shows how the bandedges corresponding to the first bandgap at J and X monotonously approach each other when the values of $(\lambda_b^0)^{-1}$ approach the vanishing condition value. The bandgap corresponding to $(\lambda_b^0)^{-1} = 2.42/\lambda_b$, which accomplishes the non-diffraction condition $S(G_1) = 0$ (see section 2.1), completely disappears since the associated bandedges are degenerated. This behavior corroborates with that obtained for the transmittance in figure 3. Moreover, this result also supports our prediction of simultaneous closing of both bandgaps in (19*a*) and (19*b*).

4. A feasible approach: metafluids

The practical realization of the SCs analyzed above clearly requires some type of engineered material because fluidlike cylinders with continuously varying acoustical properties do not exist

in nature. However, in the past few years, significant progress has been made in designing acoustic metamaterials or metafluids that have extraordinary acoustical properties. For example, it has been demonstrated [13]–[15] that arrays of solid cylinders in air behave at the long-wavelength limit like fluids whose acoustic properties can be tailored. Also, it has recently been shown that metafluids with a gradient index of refraction can be achieved by embedding solid inclusions in a fluid or gas host [6].

Therefore, by using the homogenized properties of specially designed SC, a cylinder with a radial dependence of its index of refraction $n_s(r)$ can be engineered by a metafluid consisting of a circular cluster (of dimension equal to the cylinder's diameter) made of solid cylinders embedded in the same background as the SC. Thus, a cylinder with a radially dependent $n_s(r)$ as considered by general expression (9) can be engineered by following the method described in [6]. Particularly, we consider water as the background and use a circular cluster made of lead (Pb) and air cylinders in a square arrangement. Also, it is important to remark that the radii of cylinders change from the center to the border of the cluster by applying the appropriate recipe [6].

In order to verify that the designed metafluid and the exact fluidlike cylinder have the same scattering properties, we study the scattering properties of both systems by an impinging sound wave of wavelength $25a$, where a is the lattice parameter of the array in the cluster and $R_c(=7a)$ is the radius of both the fluidlike cylinder and the cluster. While the calculation of the scattering by a cluster of rigid cylinders is a well-known problem in multiple scattering theory, the scattering by an inhomogeneous fluidlike cylinder requires a special numerical algorithm that has been developed by Cai and co-workers [16, 17].

Figures 5(a) and (b) show, respectively, the maps of the amplitude for the total acoustic pressure around a metafluid cylinder and its corresponding inhomogeneous cylinder with a refractive index profile given by $n_s(r) = \sqrt{1+3.97(r/R_c)^2}$ (black line in figure 2). The comparison of both maps shows that the metafluid represents fairly well the scattering properties of the fluidlike cylinder having continuously varying properties. Note that the agreement between pressure maps not only exists in the far-field regime but also in the near-field regime and inside the fluidlike cylinder's bulk.

The numerical experiment reported above supports the feasibility of the scatterers proposed to build the SC analyzed here. Now, in order to manipulate the bulk modulus of the background one can use the procedure described in [6] to design the background metafluid with the required bulk modulus and keep the same mass density. This manipulation of the background modulus could even be made dynamic by inserting (or removing) the arrays of cylinders defining the metafluid background and, therefore, the dynamical switching off/on of the selected bandgaps should be possible.

5. Discussion and summary

In conventional SC consisting of binary systems ($n_s \neq n_b$) the transparency (non-diffraction) condition is achieved when all the bandgaps are closed ($n_s = n_b$) and therefore, the SC becomes totally homogeneous and transparent to every wavelength passing through. Here we have shown that, in SC made of radially varying acoustic parameters $n_s(r)$, the transparency condition associated with the different bandgaps can be selectively switch on and off by tuning the acoustic parameters of either the scatterers or the background. Another possibility is by the modulation

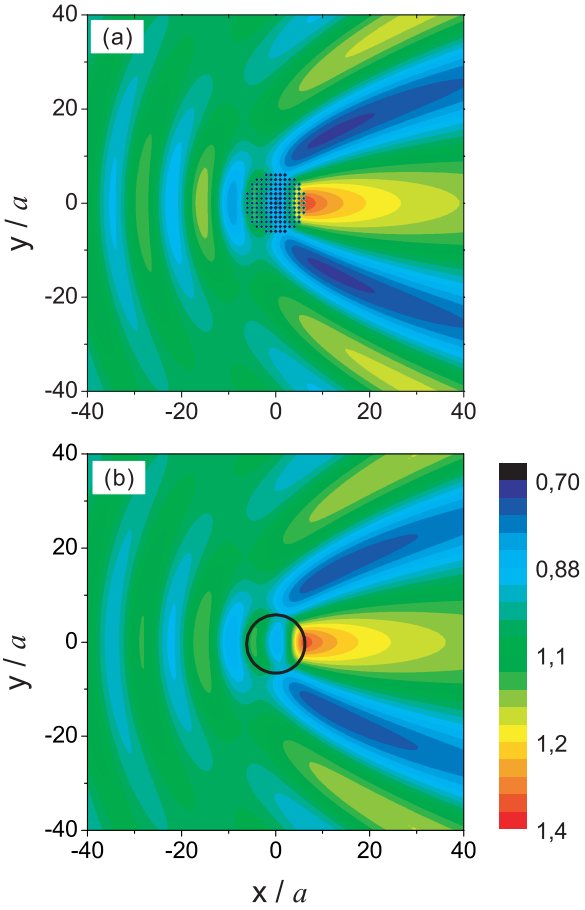

Figure 5. (a) Pressure map (amplitude) of the scattering of a sound plane wave impinging from the left to a cluster made of lead and air cylinders embedded in water (see text). The wavelength of the impinging sound is $25a$, where a is the lattice separation between cylinders in the cluster. (b) The corresponding map for the case of an inhomogeneous cylinder embedded in water and characterized by an index of the refraction profile given by $n_s(r) = \sqrt{1+3.97(r/R_c)^2}$, where $R_c = 7a$ is the cluster radius in (a). Both plots use the same color scale.

of the reciprocal lattice vectors; for example, by using a mechanical device, it would be possible to produce a uniform compression or expansion of the SC lattice. Particularly, we have analyzed in detail the case of SC in which the cylindrical scatterers and the background have the same density. For these particular systems we have given the conditions over the background modulus to obtain the transparency on the range of wavelength selectively chosen.

We have also demonstrated by numerical experiments that the scatterers with radially varying properties can be feasible to engineer by using metafluids consisting of arrays of two components cylinders. One can envisage interesting applications of having on–off selectivity switching in a SC. We hope that this proposal motivates experimental work confirming the result and producing novel acoustic devices.

Acknowledgments

The work was partially supported by the Spanish MEC under Project no. TEC2007-67239. LWC acknowledges the financial support by the US National Science Foundation under grant CMS-0510940 and supplemental funding from the International Research and Education in Engineering (IREE) program. DT acknowledges a PhD grant paid by MEC. We also thank Helios Sanchis Alepuz for useful discussions.

References

[1] Alú A and Engheta N 2005 Achieving transparency with plasmonic and metamaterials coatings *Phys. Rev.* E **72** 016623
[2] Alú A and Engheta N 2007 Plasmonic materials in transparency and cloaking problems: mechanism, robustness, and physical insights *Opt. Express* **15** 3318
[3] Velentine J, Zhang S, Zentgraf T, Ulin-Avila E, Genov D A, Bartal G and Zhang X 2008 Three dimensional optical metamaterial with negative index of refraction *Nature* **455** 376
[4] Li J and Chan C T 2004 Double negative acoustic metamaterial *Phys. Rev.* E **70** 055602
[5] Zhou X. and Hu G. 2007 Acoustic wave transparency for a multilayered sphere with acoustic metamaterials *Phys. Rev.* E **75** 046606
[6] Torrent D and Sánchez-Dehesa J 2007 Acoustic metamaterials for new two dimensional sonic devices *New J. Phys.* **9** 323
[7] Born M and Wolf E 1999 *Principles of Optics* (Cambridge: Cambridge University Press)
[8] Kittel C 1996 *Introduction to Solid State Physics* (New York: Wiley)
[9] Sakoda K 2001 *Optical Properties of Photonic Crystals* (Berlin: Springer)
[10] Cassagne D, Jouanin C and Bertho D 1996 Hexagonal photonic-band-gap structure *Phys. Rev.* B **53** 7134
[11] Yasumoto K, Toyama H and Kushta T 2004 *IEEE Trans. Antennas Propag.* **52** 2603
[12] Sanchis L, Håkansson A, Cervera F and Sánchez-Dehesa J 2003 Acoustic interferometers based on two-dimensional arrays of rigid cylinders in air *Phys. Rev.* B **67** 035422
[13] Cervera F, Sanchis L, Sánchez-Pérez J V, Martinez-Sala R, Rubio C, Meseguer F, Lopez C, Caballero D and Sánchez-Dehesa J 2002 Refractive acoustic devices for airborne sound *Phys. Rev. Lett.* **88** 023902
[14] Krokhin A A, Arriaga J and Gumen L N 2003 Speed of sound in periodic dielectric composites *Phys. Rev. Lett.* **91** 264302
[15] Torrent D, Håhansson A, Cervera F and Sánchez-Dehesa J 2006 Homogenization of two dimensional clusters of rigid rods in air *Phys. Rev. Lett.* **96** 204302
[16] Cai L-W 2004 Multiple scattering in a single scatterer *J. Acoust. Soc. Am.* **115** 986
[17] Cai L-W and Sánchez-Dehesa J 2008 Acoustical scattering by radially stratified scatterers *J. Acoust. Soc. Am.* **124** 2715